# PRACTICAL HELICAL CONE BEAM ALGORITHM FOR THE LONG OBJECT PROBLEM

JICUN HU, ROGER JOHNSON, CHRISTOPHER DAWSON

DEPARTMENT OF BIOMEDICAL ENGINEERING, MARQUETTE UNIVERSITY, USA

## INTRODUCTION

Cone beam computed tomography (CT) based on non-planar orbits has been an active area of research toward the goal of producing an exact volumetric reconstruction. To date, most reconstruction algorithms for non-planar orbits have been based on the theoretical framework of Tuy[1], Smith [2] and Grangeat[3]. Of all the investigated non-planar orbits, the helical scanning geometry is most promising for clinical application since it is easy to implement and natural for volume scanning of the body.

Currently, multi-row detectors with only a few rows (e.g. four) are widely used in clinical helical CT, and the reconstruction algorithms involved differ only slightly from the traditional fan beam methods. This approximation produces minimal artifact in the reconstruction because the cone angle is very small. In order to increase the volume scanning speed and reduce motion artifacts, and to make more efficient use of the x-ray tube output, more and more detector rows will be used. In the near future a point will be reached where the z-divergence of the beam will become non-negligible. There is a need, therefore, to develop efficient reconstruction algorithms which account properly for the cone beam scanning geometry.

Some approximate algorithms for helical cone beam tomography have been developed[4,5,6]. They are efficient and provide good temporal resolution because only full scan or half scan data are used to reconstruct a slice and the ramp filtered data remain bounded in the z direction, keeping the computational intensity low. They are approximate in nature however, and will produce artifacts when the cone angle is increased.

Practical exact helical cone beam tomography algorithms are made possible by the discovery that only the truncated data within the region on the detector bounded by the projections of the adjacent upper and lower turns of the helix are required to obtain an exact reconstruction [7,8], not the full data set as utilized in the theory developed by Tuy, Smith and Grangeat. Quasi-exact algorithms outperform approximate methods in terms of reconstructed image quality, yet some researchers have argued that exact algorithms have the disadvantages of inferior temporal resolution and increased computational intensity. We show that an exact algorithm can deliver computational efficiency and temporal resolution comparable to that achieved by approximate methods. With continued research in this area, the advantages of exact over approximate algorithms will become increasingly evident.

Exact helical cone beam tomography algorithms can be categorized as addressing the short object problem or the long object problem. For the short object problem, the axial extent of the helix is sufficient to cover the entire object, providing adequate data for a comparatively simple solution. For the more complex long object problem, the helix extends only slightly beyond the ROI. It is much more difficult to solve than the short object problem due to the data contamination issue. From a clinical standpoint, a solution to the long object problem is required since only a portion of the patient should be scanned to provide accurate images of the finite volume of interest. Tam[7] first provided a solution for the long object problem, but his algorithm required two circular orbits at the end of helix which is undesirable in practice. Several exact algorithms for the long object problem have been developed which do not require the circular orbits, but reconstruct the ROI using only the helical orbit data[9,10,11].

In this paper, we present a new solution to the long object problem using helical data only. It is based on the method developed by Kudo, Noo and Defrise[8]. We invoke the concept of accessory paths with upper and lower virtual detectors having infinite axial extent. We show that our approach has the advantages of ease of implementation, good temporal resolution and computational efficiency. The algorithm possesses the filtered backprojection structure, which is very desirable for practical implementation.

## ALGORITHM

We propose an algorithm to solve the long object problem for helical cone beam tomography using accessory paths with virtual detectors of infinite axial extent.

Fig. 1 illustrates the data acquisition geometry. The source path $\vec{a}(\theta)$ is a short helical segment of pitch $2\pi h$ and radius R defined by (1), containing a primary helix (the solid path), a top accessory helix (top dotted path) and a bottom accessory helix (bottom dotted path) around a long object $f(x,y,z)$ (the cylinder).

$$\vec{a}(\theta) = (R\cos\theta, R\sin\theta, h\theta)^T, \qquad (1)$$

where $\theta$ is the rotation angle of the helix.

The detector is normalized to the iso-center and its coordinate system is defined by unit vectors $\vec{\xi}_u$ and $\vec{\xi}_v$:

$$\vec{\xi}_u = (-\cos\eta\sin\theta, \cos\eta\cos\theta, \sin\eta)^T \quad (2)$$

$$\vec{\xi}_v = (\sin\eta\sin\theta, -\sin\eta\cos\theta, \cos\eta)^T \quad (3)$$

$$\eta = \arctan(h/R) \quad (4)$$

$\vec{\xi}_u$ is parallel to the helix tangent.

Our objective is to reconstruct a slice (the shaded ellipse in Fig. 1) from the data collected on the source helix. From short object problem theory, we know that it is impossible to exactly reconstruct the slice without scanning the whole object due to the data contamination problem.

Our approach employs three different types of detector. For the data collected from the primary path, we have a masked detector (Fig. 2b) with the top and bottom boundaries given by[8]:

$$V_r(u_r) = h(1+\frac{u_r^2}{R^2})[\frac{\pi}{2} - \arctan(\frac{u_r}{R})] \quad (5)$$

$$V_r(u_r) = -h(1+\frac{u_r^2}{R^2})[\frac{\pi}{2} + \arctan(\frac{u_r}{R})] \quad (6)$$

where $(u_r, v_r)$ is the rotated coordinate system defined by:

$$u_r = u\cos\eta - v\sin\eta \quad (7)$$

$$v_r = u\sin\eta + v\cos\eta \quad (8)$$

so that $u_r$ is horizontal.

For the data collected from the top accessory path, we use a detector (Fig. 2a) with no boundary on the top and with a boundary at the bottom defined by (6) in order to capture the entire upper portion of the object. For the data collected from the bottom accessory path, we use a detector (Fig. 2c) unbounded at the bottom with a boundary at the top defined by (5) in order to capture the entire lower portion of the object.

Before explaining our algorithm, we revisit an important and remarkable property of the filtered masked projection discovered by Kudo *et al.* [8]. Namely, the result of filtering the masked data can be represented as:

$$g^F(u,v,\theta) = g^F_{bounded}(u,v,\theta) + g^F_{unbounded}(u,v,\theta). \quad (9)$$

The bounded term results from ramp filtering the data within the mask and the unbounded term results from the unbounded filtering of the boundary data. This property is the key to an understanding of our algorithm. According to the above property, we know that for the central detector (the standard PI detector, Fig. 2b), data on both boundaries will contribute to the unbounded part of the filtering result, but for the upper detector (Fig. 2a), only the data on the bottom boundary will contribute to the unbounded term and for the lower detector (Fig. 2c), only the data on the top boundary will contribute to the unbounded term.

The following conditions on the primary path and accessory paths must be met in order for our algorithm to succeed. The primary path must be long enough so that the ramp filtered part of the projections collected from the accessory paths do not contribute to the reconstructed slice. The accessory paths (the dotted paths in Fig. 1) must be of length $(\pi + 2\arcsin(\frac{r}{R}))$ at both ends of the primary path, where r is the FOV radius. When these conditions are met, we can obtain the Radon derivatives needed to reconstruct every point in the slice based on the whole object. A typical data combination is shown in Fig. 3. Notice that for points on the accessory paths, one end of the source rays' envelope opens to infinity because we employ a virtual detector of infinite extent above and below the slice. But remember, the infinite detector is virtual and the unlimited data is not available in practice. Fortunately, because of the filtering property we mentioned earlier, only the data on the bottom boundary of the upper virtual detector and the data on the top boundary of the lower virtual detector will become unbounded after filtering and contribute to the reconstruction of the slice. The ramp filtered portion of the filtered projection from the accessory paths will not contribute to the reconstructed slice. Therefore, only the data on the boundaries of the upper and lower virtual detectors are required for exact reconstruction of the slice. These data are available from the primary path itself due to the property that the integral over a PI line can be accessed from either of the two source points that define the PI line (Fig. 4). Thus, the slice of interest can be reconstructed from the primary path data alone.

Explicitly, we can reconstruct the slice using the following three steps:

- Fully filter the projections (bounded term + unbounded term) obtained from the primary path and backproject the filtered results into the slice.
- Obtain the boundary data for the accessory paths, do the filtering (unbounded term only) and backproject the result into the slice.
- Add these two contributions to get a fully reconstructed slice.

If we need to reconstruct an ROI in a long object, we can reconstruct every slice in the ROI using the above approach.
Our algorithm has the following advantages:

- It is local. Every filtered projection contributes only to a few slices and it is not necessary to extend it to cover the entire ROI. This property makes the computational efficiency comparable to the approximate methods.
- It has good temporal resolution: In order to fully reconstruct a slice with the parameters used in medical CT, we require only about one turn of helical data.
- It is relatively easy to implement, requiring only slight modifications to the short object implementation.
- Only helical data is needed.
- It possesses the filtered backprojection structure.

The algorithm can be made global if the filtered projection is extended sufficiently to contribute to the reconstruction of the whole ROI, but this increases the computational intensity and reduces the temporal resolution.

The pitch of the accessory paths can vary. Our algorithm is equivalent to Kudo's virtual circle algorithm [10] when the pitch of the accessory paths becomes 0 although our derivation differs from that of Kudo. We calculate Radon derivatives based on the whole object while Kudo calculated Radon derivatives based on the ROI defined by the two virtual circles.

In our implementation we chose the pitch of the accessory paths to be the same as that of the primary path making the mask B invariant which results in a single form of the boundary term. This makes it easier to localize the reconstruction and to implement the algorithm than is the case using Kudo's virtual circle approach [10].

## SIMULATION RESULTS

We reconstructed the 3D Shepp-Logan phantom[12] (Fig. 5, display window [1.01 1.04]) and a disk phantom[8] (Fig. 6, display window [0.3 1.7]) to test the ability of the algorithm to reconstruct low contrast objects and objects with high frequency components in the z direction, respectively. We added two homogeneous cylinders at both ends of the phantoms to simulate the long objects. As demonstrated in the figures, both phantoms were reconstructed with satisfactory results.

## ACKNOWLEDGEMENTS

We acknowledge support from the Whitaker Foundation, the Keck Foundation, the Falk Medical Trust, the Rose E. Bagozzi Professorship, NHLBI HL-19298, and the Veterans Administration.

## REFERENCES

[1] H.K. Tuy, "An inversion formula for cone-beam reconstruction", SIAM J. Appl. Math., vol. 43, pp. 546-554,1983.

[2] B.D. Smith, "Image Reconstruction from cone-beam projections: necessary and sufficient conditions and reconstruction methods", IEEE Trans. Med. Imaging, vol. MI-4, pp.14-25,1985.

[3] P. Grangeat, "Mathematical framework of cone beam 3D reconstruction via the first derivative of the Radon transform" in Mathematical Methods in Tomography, Lecture Notes in Mathematics 1497, G.T. Herman, A.K. Louis, F. Natterer, eds. New York: Springer-Verlag, 1991, pp. 66-97.

[4] G. Wang, Y.Liu, T.H. Lin, P-C. Chen and D.M. Shinozaki, "A general cone-beam reconstruction algorithm", IEEE Trans. Med. Imaging, vol. 12, pp.486-496, 1993.

[5] H. Turbell and P-E. Danielsson, "Non-redundant data capture and highly efficient reconstruction for helical cone-beam CT", Conf. Record of 1998 IEEE Medical Imaging Conference, pp.1424-1425, 1998.

[6] F. Noo, M. Defrise and R. Clackdoyle, "Single-slice rebinning method for helical cone-beam CT", Phys. Med. Biol., vol. 44, pp. 561-570, 1999.

[7] K.C. Tam, S. Samarasekera and F. Sauer, "Exact cone-beam CT with a spiral scan", Phys. Med. Biol., vol. 43, pp. 1015-1024, 1998.

[8] H. Kudo, F. Noo and M. Defrise, "Cone-beam filtered-backprojection algorithm for truncated helical data", Phys. Med. Biol., vol. 43, pp. 2885-2909, 1998.

[9] M. Defrise, F. Noo and H. Kudo, "A solution to the long object problem in helical cone beam tomography", Phys. Med. Biol., vol. 45, pp. 1-21, 2000

[10] H.Kudo, F. Noo and M. Defrise, "Quasi-exact filtered backprojection algorithm for long object problem in helical cone beam tomography", IEEE Trans. Med. Imaging, vol.1, pp. 902-921, 2000

[11] S. Schaller, F. Noo, F.Sauer *et al.*, "Exact Radon rebinning algorithm for the long object problem in helical cone beam CT", IEEE Trans. Med. Imaging, vol. 19, pp. 361-375, 2000.

[12] C. Jacobson, "Fourier Method in 3D reconstruction from cone-beam data", Ph.D. Thesis, Linkoping University, 1996.

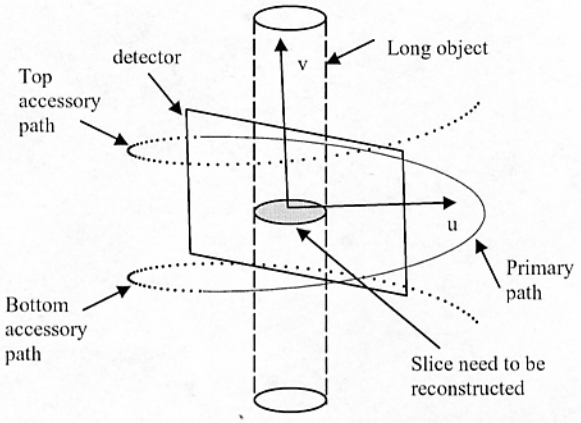


Fig. 1

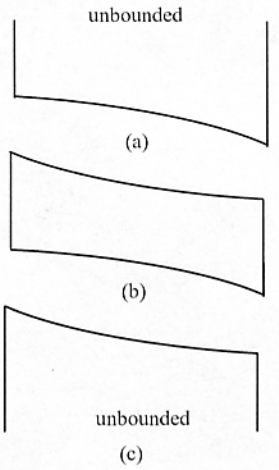


Fig. 2

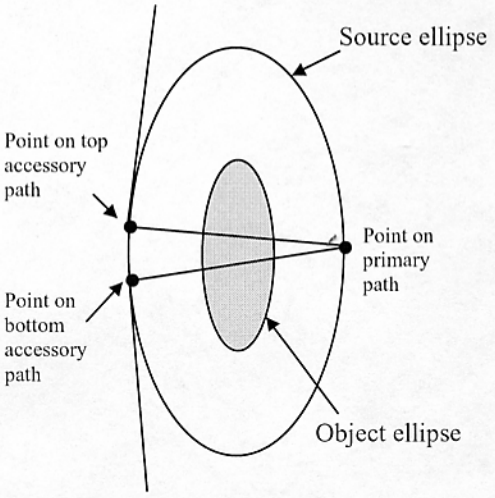


Fig. 3

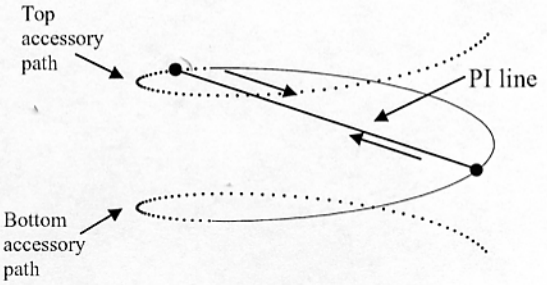


Fig. 4

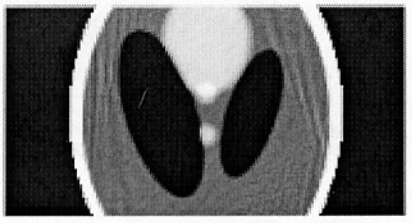

Fig. 5

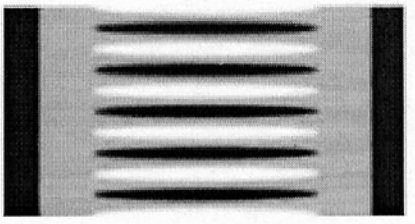

Fig. 6